Structural Chemistry (2022) 33:91–100
https://doi.org/10.1007/s11224-021-01809-8

ORIGINAL RESEARCH

Protonated MF_6^- (M=Au, Ir, Os, Re, Ta, W) behave as superacids and are building blocks of new class of salt

Anoop Kumar Pandey [1] · D. V. Shukla [2] · Vijay Narayan [3] · Vijay Singh [4] · Apoorva Dwivedi [5]

Received: 4 May 2021 / Accepted: 5 July 2021 / Published online: 26 August 2021

Abstract

Novel strong superacids HMF_6 (M=Au, Ir, Os, Re, Ta, W) are proposed and are investigated with the help of DFT/B3LYP method and SDD basis set for 5d transition metals as well as 6-311++G (d) basis set for H and F atoms. These HMF_6 superacids are composed with Brønsted/Lewis (MF_5/HF). The stabilities of HMF_6 are discussed with the help of structure, dissociation energy through HF channel, and normal mode analysis. The ΔE_{disso}>0 shows that all HMF_6 superacids are energetically stable through HF dissociation channel. The gas phase acidity of HMF_6 has been calculated by the Gibbs free deprotonation energy. All species of HMF_6 belong to superacids having smaller deprotonation energy; 100% concentrated H_2SO_4 acids however predicted ΔG_{dep} of $HAuF_6$, is nearly equal to ΔG_{dep} of $HSbF_6$. The strength of acidity of HMF_6 is closely related to vertical detachment energy (VDE) of their corresponding superhalogen anions MF_6^-. This study provide appropriate path to design new class of superacids which is more acidic than $HSbF_6$. We have also modelled and discussed supersalt by the interaction of Li with MF_6 superhalogen.

Keywords Superacid · Gas phase acidity · Superhalogens · VDE

Introduction

Superhalogens with electron affinity (EA) and vertical detachment energy (VDE) values exceed than halogen, which got much attention from last four decades. These abnormal complexes are presented by a central atom decorated with electronegative legends which lead to increase their EA greater than Cl. The superhalogens play an important role in chemical and health industry as they purify air [1, 2]. In the last decade, some useful application of superhalogen, e.g., safe electrolytic salts for lithium ion batteries [3, 4] and efficient materials for hydrogen storage area, came into light [5]. In recent years, this is noticed that protonation of superhalogen guides formation of superacids [6]. The concept of superacids was introduced by Hall and Conant in 1927 [7]. The chemistry of superacids was developed by Olah and Hogeveen [8, 9] and in 1970, Gillespie [10, 11] gave the scientific definition of superacids. According to him, superacids are those species which are more acidic than 100% H_2SO_4 or with Hammett acidity function smaller than −12. Olah et al. reported the first magic acids (HSO_3F:SbF_5) with mixture of 1:1 which goes under the criteria of superacid [12]. Superacids are mainly classified as Lewis/Brønsted and conjugate Brønsted/Lewis. Recently, most of the strong superacids are reported by combination of conjugate Brønsted/Lewis [13, 14]. Currently, $HSbF_6$ is considered to be the strongest superacid as it is 10^9 times more acidic than 100% H_2SO_4 [15]. This $HSbF_6$ superacid can also be expressed as a combination of (SbF_5/HF) SbF_5 Lewis acid and HF Brønsted acid. Koppel et al. theoretically predicted that $F(SO_3)_4H$, FSO_3SbF_5H, and $HAlCl_4$ are stronger acids on basis of Gibbs free energies of deprotonation (ΔG_{dep}) which were similar to one of the strongest superacid $HSbF_6$ (255.5 kcal/mol) [6]. At this place, it is necessary to point out that ΔG_{dep} is the most important factor for describing the gas phase acidity of any species. The protonation of anion of superhalogen Al_nF_{3n+1} (n=1–4) easily relied as HF/AlnF3n

✉ Apoorva Dwivedi
apoorvahri@gmail.com

1 Department of Physics, K. S. Saket P G College, Ayodhya, India

2 Department of Physics, GLA University, Mathura, India

3 Maa Anjani Mahavidhyala, Jaganpur Dehat, India

4 Department of Physics, University of Dodoma, Dodoma, Tanzania

5 Department of Applied Science and Humanities, Seth Vishambhar Nath College of Engineering, Research and Technology, Barabanki, India

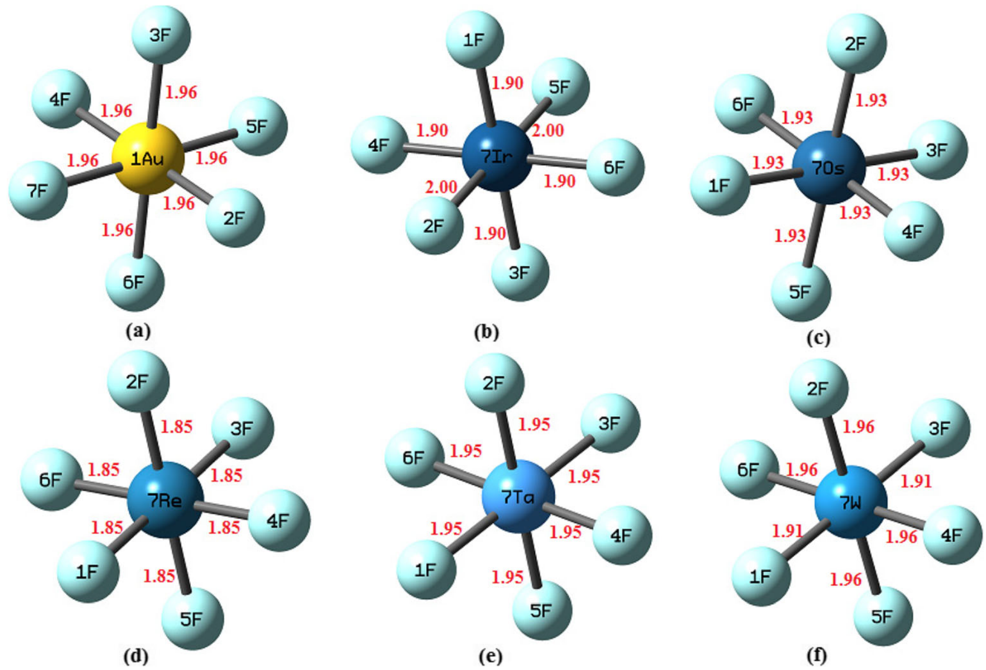

Fig. 1 Optimized structure of MF_6 anion along with bond length (in A°)

[16] and their gas phase acidity exceed to $HSbF_6$ for n=4. In similar fashion, protonation of anion of superhalogen In_nF_{3n+1}, Sn_nF_{4n+1}, and Sb_nF_{5n+1} (n=1–3) easily relied as HF/In_nF_{3n}, HF/Sn_nF_{4n}, and $HF/SbnF_{5n}$ respectively and shows more acidity than $HSbF_6$ [17]. Ambrish et al. have reported that protonation of $B(BF_4)_4$–, $B(AlF_4)_4$–, and $Al(BF_4)_4$– as well as $Al(AlF_4)_4$– superhalogens shows more acidic behavior than $HSbF_6$ in the gas phase [18]. In the above example, it is noticed that these superhalogens contain F as ligands and rely to HF (Brønsted acid) by protonation. The role of HF (Brønsted acid) in increasing acidity of superacids is reported [19]. This was also reported that successive attachments of HF to Lewis acid gradually increase gas phase acidity [20]. So it is difficult to say that the presence of HF enhances protonation of superhalogen or this is an intrinsic property of superhalogen. Recently, it is reported that protonation of halogen-free anions superhalogen B_nH_{3n+1}(n=1–5) gives new class of superacids which have no role of HF (Brønsted acid) so superacidic behavior of complex is an intrinsic property of superhalogen [21]. Indeed, acidity of any superacidic should relate to electronic stability of their anionic superhalogen part. The VDE is an important parameter to determine electronic stability of anionic part of superhalogen. This is also reported that VDE of anions of superhalogen as well as gradually increases the number of ligands that are directly related to gas phase acidity. To verify this, we fix a number of ligand of six in present communication and we choose some hydrogenated complex of AuF_6, IrF_6, OsF_6, ReF_6, TaF_6, and WF_6 series noticed that they really belong to superacid family. In this study, we again find a correlation in between VDE and interaction energy of HF-MF_5 with acidity of superacids. We reveals that the acidity of these HMF_6 (M=Au, Ir, Os) species are comparable to the strongest superacids $HSbF_6$. We also hope that our study provides new path for designing new superacids in the future. At last, we have also modelled and discussed supersalt by the interaction of Li with MF_6 superhalogen.

Table 1 Calculated various parameters of MF_6^- by using DFT/SDD/6-311++G (d) basis set

S.N.	Spe.	Sym.	Exp. bond leng. (A^0)	VDE (eV)	VDE[35] (eV)	ADE (eV)	Exp. (ADE)	Other cal.	Dissociation F^-(eV)
1	AuF_6^-	O_h	1.899[41], 1.874[40], 1.861[44], 1.890[43]	8.59	8.52	8.44	–	8.20[26], 8.1[36], 9.56[38]	4.47
2	IrF_6^-	D_{4h}	1.879[40], 1.875[42]	6.42	5.90	6.25	6.50±0.38[33]	5.99[28], 5.34[39], 7.2[37]	4.87
3	OsF_6^-	D_{4h}	1.872[40], 1.879[40]	8.22	6.27	6.18	5.93±0.28[33]	5.92[29]5.55[39], 6.0[36]	5.02
4	ReF_6^-	O_h	1.863[41]	7.35	4.99	5.24	>3.80[34]	4.58[27], 4.50[39], 4.8[36]	2.32
5	TaF_6^-	O_h	–	4.93	–	8.41	–	–	4.84
6	WF_6^-	D_{4h}	–	3.76	3.44	3.74	3.50±0.1[31], 3.36[32]	3.16[30], 3.34[39], 3.85[37]	4.74

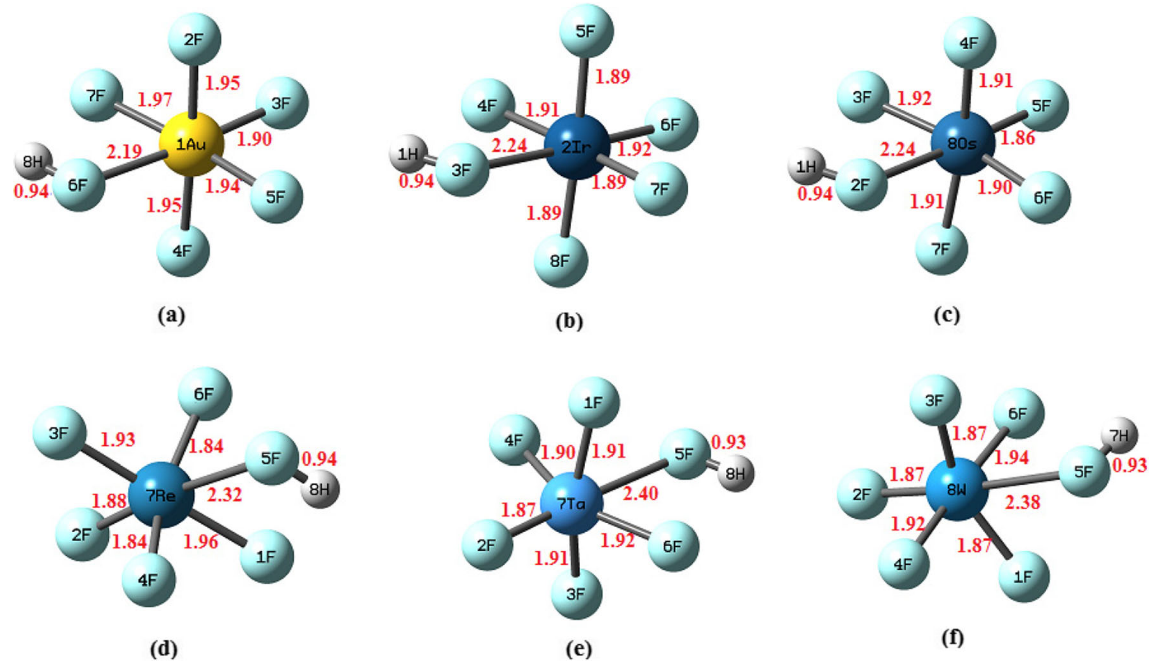

Fig. 2 Optimized structure of HMF_6 along with bond length (in A^o)

Fig. 3 Optimized structure of MF_5 neutral along with bond length (in A^o)

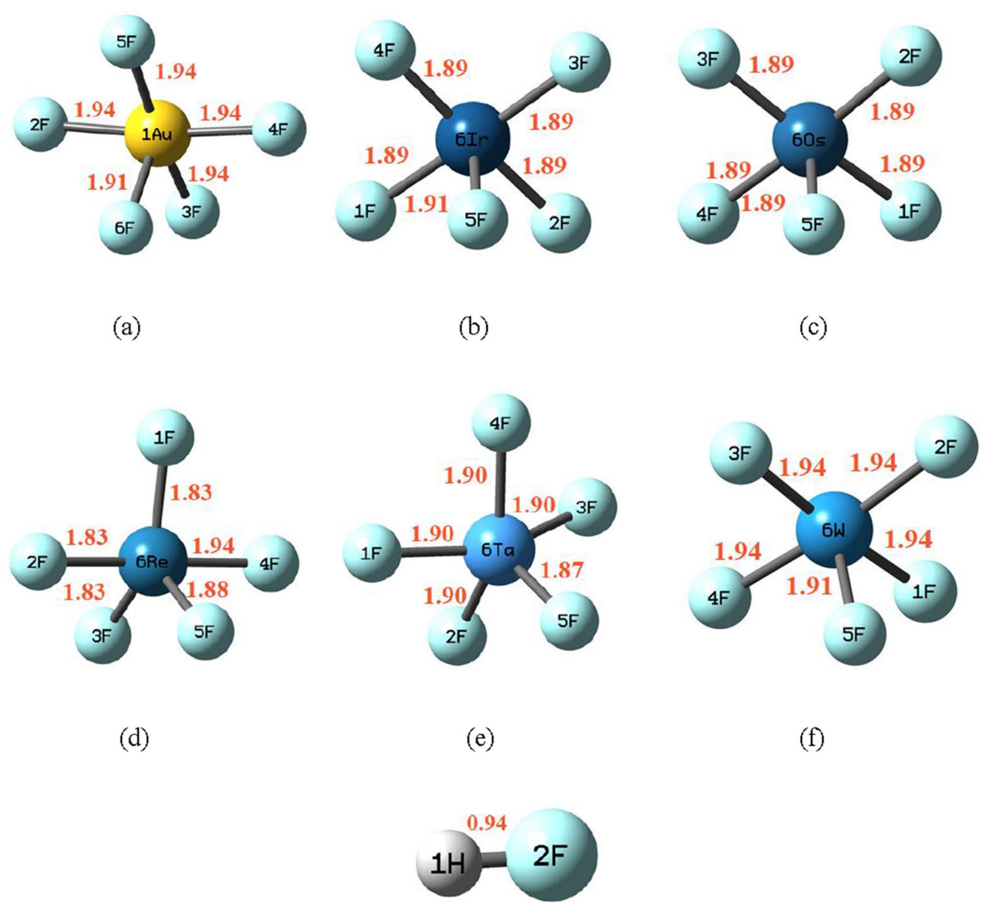

Table 2 Calculated various parameters of HMF_6 by using same level theory

Species	ΔH (Kcal/mol) $HMF_6 \rightarrow H^+ + MF_6^-$	ΔG_{depro}(kcal/mol)	E_{ele} (eV)	ΔE_{disso} (eV) $HMF_6 \rightarrow HF + MF_5$
$HAuF_6$	244.44	260.48	2.76	0.55
$HIrF_6$	257.35	273.01	2.20	0.15
$HOsF_6$	245.13	264.86	2.71	0.59
$HReF_6$	246.35	267.35	2.19	0.86
$HTaF_6$	270.63	274.19	2.17	0.29
HWF_6	258.40	276.16	2.13	0.25

Computational details

All anionic hexafluorides and their corresponding protonated structure are fully optimized with the help of DFT/B3LYP method using G09 program package [22]. In this study, we have employed SDD basis set for 5d transition metals and 6-311++G (d,p) basis set for H and F atoms. All structures are optimized without any symmetry constrains. The above method and basis sets are also employed in previous studies.

The vibrational analysis is performed to ensure that all structures belong to true minima. The vertical detachment energy of MF_6^- is calculated by energy difference between optimized MF_6^- structure to single point energy calculation of corresponding neutral MF_6:

$$\mathrm{VDE} = E\,(MF_6^-)_{\mathrm{optimized}} - E\,(MF_6)_{\text{ single point}}$$

The acidity of HMF_6 in gas phase is defined by change in Gibbs free energy of deprotonation reaction.

$HMF_6 \rightarrow H + MF_6^-$ at T=298.15K is calculated by the following reaction:

$$\Delta G_{acid} = \Delta G\left[MF_6^-\right] + \Delta G\ [H^+] - \Delta G\ [HMF_6]$$

where $\Delta G\,[H^+] = -6.28$ kcal/mol is taken from literature [23].

The HOMO and LUMO are plotted with the help of Gauss View 5.0 [24]. Gauss sum 3.0 is used for PDOS plot of $LiMF_6$ supersalts.

Result and discussion

In this paper, we have discussed the formation of superacids by protonation of anions of transition metal hexafluoride MF_6^-. So, we have performed our calculation on MF_6^- / HMF_6 containing representative 5d transition metal such as Au, Ir, Os, Re, Ta, and W. Our study is based on the following criteria:

(1) Both MF_6^- /HMF_6 are chemically and thermodynamically stable.
(2) To establish superacidic behavior of HMF_6, Gibbs free energy should not exceed 300kcal/mol.
(3) The structure HMF_6 is intact with two noticeable parts of HF/MF_5.
(4) Finally, see the relation between VDE of MF_6^- with deprotonation energy of HMF_6.

Let us discuss these criteria one by one for all six entities:

MF_6^-

First of all, we discuss the structure of conjugate base anions (MF_6^-) in HMF_6 superacids. For this, we have considered all possible geometry of MF_6^- and after geometry optimization, most stable geometries of MF_6^- are displayed in Figure 1. We have also optimized most stable geometry of MF_6^- at various multiplicities by using combination DFT/B3LYP method and SDD/6-311++G (d, p) basis set. We have calculated lowest

Table 3 Mullikan atomic charges on various atoms and subunits of HMF_6 by using same level theory

Species	HF subunit		Charge on H	Charge on MF_5	Charge on HF	Charge on MF5+F
	Atom	Charge				
$HAuF_6$	F_3	0.053551e	0.338329e	−0.391881e	0.391880e	−0.338330e
$HIrF_6$	F_6	−0.135375e	0.472217e	−0.336841e	0.336842e	−0.472216e
$HOsF_6$	F_2	−0.210527e	0.475590e	−0.265062e	0.265063e	−0.475589e
$HReF_6$	F_5	−0.267365e	0.470875e	−0.203510e	0.203510e	−0.470875e
$HTaF_6$	F_5	−0.115837e	0.334944e	−0.219107e	0.219107e	−0.334944e
HWF_6	F_5	−0.126902e	0.351018e	−0.224116e	0.224116e	−0.351018e
HF	F_2	−0.290611e	0.290611e	–	0.000000e	

Table 4 Some electronic parameters of HMF_6 calculated by using combination of DFT/B3LYP method and SDD/6-311++G (d) basis set

Species	μ(D)	I.P.(eV)	η(eV)	EA(eV)	χ(eV)	ΔE_{gap}(eV)
$HAuF_6$	3.95	11.18	1.55	8.08	9.63	3.10
$HIrF_6$	5.34	9.58	0.81	7.97	8.78	1.61
$HOsF_6$	4.03	9.20	1.18	6.85	7.19	2.35
$HReF_6$	4.73	7.10	0.64	5.82	6.46	1.28
$HTaF_6$	2.50	11.54	5.48	3.43	4.06	8.11
HWF_6	3.53	7.35	1.32	4.71	6.03	2.64

energy conformers ofHMF_6^-/MF_6^- at various multiplicity and relative energies presented in supplementary Table 1. In all HMF_6^-/MF_6^-, Au, Ir, Re, and Ta show odd multiplicity; however, the rest Os and W show even multiplicity. The lowest energy occurs at a singlet electronic state for Au and Ta; however, Ir and Re occur at a triplet state. In even multiplicity state, Os shows the lowest energy at doublet however W at quartet. So we have performed calculations on these states. The AuF_6^-, TaF_6^-, WF_6^- shows octahedral symmetry O_h; however, IrF_6^-, ReF_6^-, OsF_6^- shows D_{4h} symmetry. The calculated bond lengths of M-F in MF_6^- are well matched with previous calculation [25–29]. The calculated ADE of MF_6^- are also well matched with experimental values [30–33]. The calculated VDE and ADE of MF_6^- (Table 1) are nearly matched with previously calculated VDE of corresponding species [33] and ADE values respectively [34–37]. The calculated VDE and ADE of MF_6^- re-established their superhalogenic behavior [38–42]. The dissociation of MF_6^- through F^- channel are calculated by:

$$\Delta E_{disso} = E(MF_5) + E(F^-) - E(MF_6^-)$$

The OsF_6^- shows the highest dissociation energy (5.02eV) among all species; however, ReF_6^- has the lowest dissociation energy (2.32eV). The calculated dissociation energy $\Delta E_{disso>0}$ of MF_6^- shows the stability of hexafluoride anion dissociation through F^- channel. The numbers of theoretical studies have predicted the dissociation energy through F channel having higher value as compared with dissociation through F^- channel [26–30] which shows that the extra charge has been carried by MF_5^- rather than F^-.

HMF_6

To study HMF_6 (M=Au, Ir, Os, Re, Ta, W), we have modelled all possible initial structures. However after optimization, lowest energy of HMF_6 corresponds to those structures in which one of F atoms interact with H atom and displayed in Fig. 2. Again to find the most stable geometry, we have run these structures at a different multiplicity employed DFT method and SDD basis set for 5d transition metals and 6-311++G (d,p) basis set for H and F atoms and their relative energy are listed in supplementary Table 1. All calculations are performed at the lowest energy structure. The optimized HMF_6 structures have no symmetry. From Fig. 2, it is obvious that there exist HF moieties in $HMF_{6.}$ This HF moieties weakly interact with central metal (Au, Ir, Os, Re, Ta, W) in HMF_6. So HMF_6 can be expressed as AuF_5/HF, IrF_5/HF, OsF_5/HF, ReF_5/HF, TaF_5/HF, and WF_5/HF. In order to explore this, we further optimized these components of HMF_6 and displayed in Fig. 3. This can be also verified by using NBO charge analysis. The calculated Mullikan atomic charges on both (MF5/HF) subunits are collected in Table 3. The atomic charges on both subunits are nearly equal means HF subunit transfer charge to MF_5 subunits. The magnitude of charge transfer from HF to MF_5 subunits is in order of 0.0001e so they bind with weak electrovalent bond and hence HMF_6 can be written as combination MF_5/HF subunits. The calculated bond lengths of M-F in MF_5 are well matched with previous studied [38–42]. The calculated bond length of H-F by DFT/6-311++G (d, p) method is well matched with experimental result. The H-F bond length calculated by using combination of DFT/B3LYP method SDD/6-311++G (d, p) and basis set in HMF_6 lies in between 0.94A^0 and 0.93A^0 and is matched with H-F bond length in free H-F molecule. However, the distance of HF species from central metal are in this order: $HAuF_6$(2.19A^0) <$HIrF_6$(2.24A^0)=$HOsF_6$(2.24A^0) <$HReF_6$(2.32A^0) <HWF_6(2.38A^0)<$HTaF_6$(2.40A^0).

To check stability of HMF_6 against dissociation through HF channel, we also calculate dissociation energy using the following formula:

$$\Delta E_{diss} = E(MF_5) + E(HF) - E(HMF_6) \text{ where M}$$
$$= \text{Au, Ir, Os, Re, Ta, W}$$

The calculated dissociation energies by using DFT/6-311++G and SDD/6-311++G (d) basis set are listed in Table 2. One can easily see that $\Delta E_{diss>0}$ for all species shows that these HMF_6 are stable against dissociation through HF channel. The calculated dissociation energy is HWF_6 followed by $HAuF_6$ through HF dissociation channel having a larger value than other species.

Deprotonation energy of HMF_6

In order to analyze gas phase acidity of HMF_6, we have calculated deprotonation energy (ΔG_{dep}) of HMF_6 species by using DFT/B3LYP method and SDD/6-311++G (d) basis set. The calculated deprotonation energies of HMF_6 are listed in Table 2. The calculated ΔG_{dep} values of all HMF_6 are smaller than ΔG_{dep} value of H_2SO_4 (303kcal/mol) which suggests that these HMF_6 species are superacids. The calculated ΔG_{dep} (260.48kcal/mol) of $HAuF_6$ is nearly matched with the corresponding value reported by Marcin Czapla (259.5kcal/mol) [43] and also comparable to ΔG_{dep} of $HSbF_6$ (261kcal/mol). All HMF_6 except HWF_6 are more acidic than $HTaF_6$ (274.6kcal/mol) as reported by Koppel et al. [6] and calculated deprotonation energy of $HTaF_6$ is well matched with ΔG_{dep} value as reported by Koppel et al. To check reliability of our methods, we have calculated ΔG_{dep} of well-known superacid $HSbF_6$ by DFT/B3LYP method and SDD/6-311++G (d) basis set. The calculated value of ΔG_{dep} of $HSbF_6$ by DFT/B3LYP method and SDD/6-311++G (d) basis set (262.76kcal/mol) shows only 1–2 kcal/mol difference which prove the reliability of our method. The variation of deprotonation energy according to $HAuF_6$<$HIrF_6$ <$HOsF_6$ <$HReF_6$ <$HTaF_6$<HWF_6 and acidity of HMF_6 varies inversely with deprotonation energy of HMF_6.

Let us see a closer insight of mechanism of deprotonation by using NBO charge analysis of HMF_6 species. The calculated charge on H atom (0.290611e) is the same but opposite as F atom (−0.290611e) in HF by using combination of DFT/B3LYP method and 6-311++G (d, p) basis set. In similar fashion, charges on MF_6 unit and H atom are the same but with higher magnitude in HMF_6 (Table 3) as compared with HF. In HMF_6 species, H atom faces more deficiency of charges as compared with F atom in HF. In this way, HMF_6 can be written as HF/MF_5 of which again HF relies to H^+ easily as compared with free HF species which shows more electrovalent character. In this way, the strength of acidity of any HMF_6 species is directly related with electronic stability of their corresponding superhalogen anions. In Fig. 4, we have plotted a correlation graph in between VDE of MF_6^- and acidity (Gas Phase) of HMF_6. The correlation follows a linear equation y=0.0498x+3.44 with correlation factor R^2=0.93 showing a fair correlation in between that VDE of MF_6^- with acidity of their protonated species as reported by Ambrish et al. [21]. Some deviation occurs in this linear correlation due to unusable behavior of heavy transition metal hexafluoride.

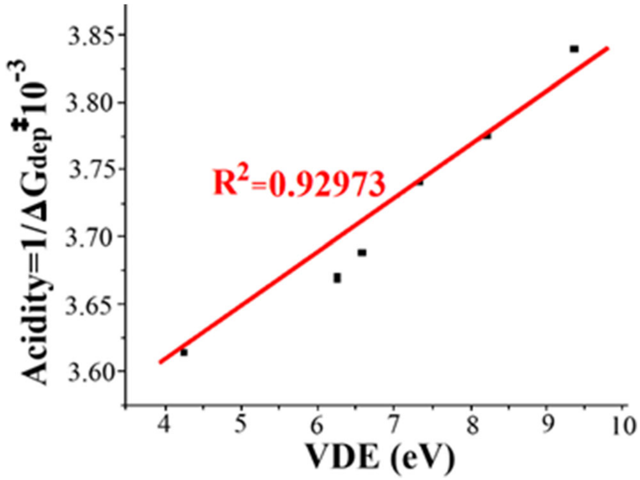

Fig. 4 Correlation graph in between VDE and acidity

Electronic properties of HMF_6

Some electronic parameters of HMF_6 are also calculated by DFT/B3LYP method and SDD/6-311++G (d) basis set which are listed in Table 4. The HOMO is known as the highest occupied molecular orbitals and primarily acts as a donor; however, LUMO is the lowest unoccupied molecular orbital and primarily acts as an acceptor. The energy difference in between HOMO and LUMO plays an important role for examining chemical reactivity of any species. The HOMO and LUMO plots of HMF_6 species are shown in Fig. 5. The LUMO covered over whole species; however; HOMO covered over whole species except HF Bronsted acid. Note that HMF_6 superacids can be expressed as MF_5/HF. The calculated E_{gap} for HMF_6, calculated by DFT/B3LYP method and SDD/6-311++G (d) basis set, are listed in Table 4. The E_{gap} values for HMF_6 are much lower than E_{gap} of HF (11.40eV); however, E_{gap} value of $HTaF_6$ is comparable with E_{gap} of HF. The E_{gap} of HMF_6 varies according to $HReF_6$<$HIrF_6$<HWF_6<$HOsF_6$<$HAuF_6$<$HTaF_6$. In this way, $HReF_6$ is most reactive than other species; however, $HTaF_6$ is less reactive than all species. The dipole moments of any species are closely related to their geometry and electronic structure.

Salt formation

Strong acids and strong bases from salt, superacid, and superbases also form supersalt. In this section, we have modelled supersalt by using HMF_6 superacids. For this, we have considered several possible geometries of $LiMF_6$ supersalts and after geometry optimization, one can note that the most stable conformer is displayed in Fig. 6. The geometry of MF_6 structure is distorted and Li binds with its two F atoms in $LiMF_6$ supersalt. The calculated bond lengths are displayed with optimized geometry of $LiMF_6$ (Fig. 6).The bond lengths of Li-F lie in between 1.83 A^0 and 1.89A^0. The calculated value of Ir-F (1.89–2.04A^0) is well matched with the experimental value (1.879 A^0/1.875 A^0) [28, 44]. The vibrational frequencies of $LiMF_6$ are positive to ensure that $LiMF_6$ are stable. The calculated dissociation energy of $LiMF_6$ through LiF channel is calculated:

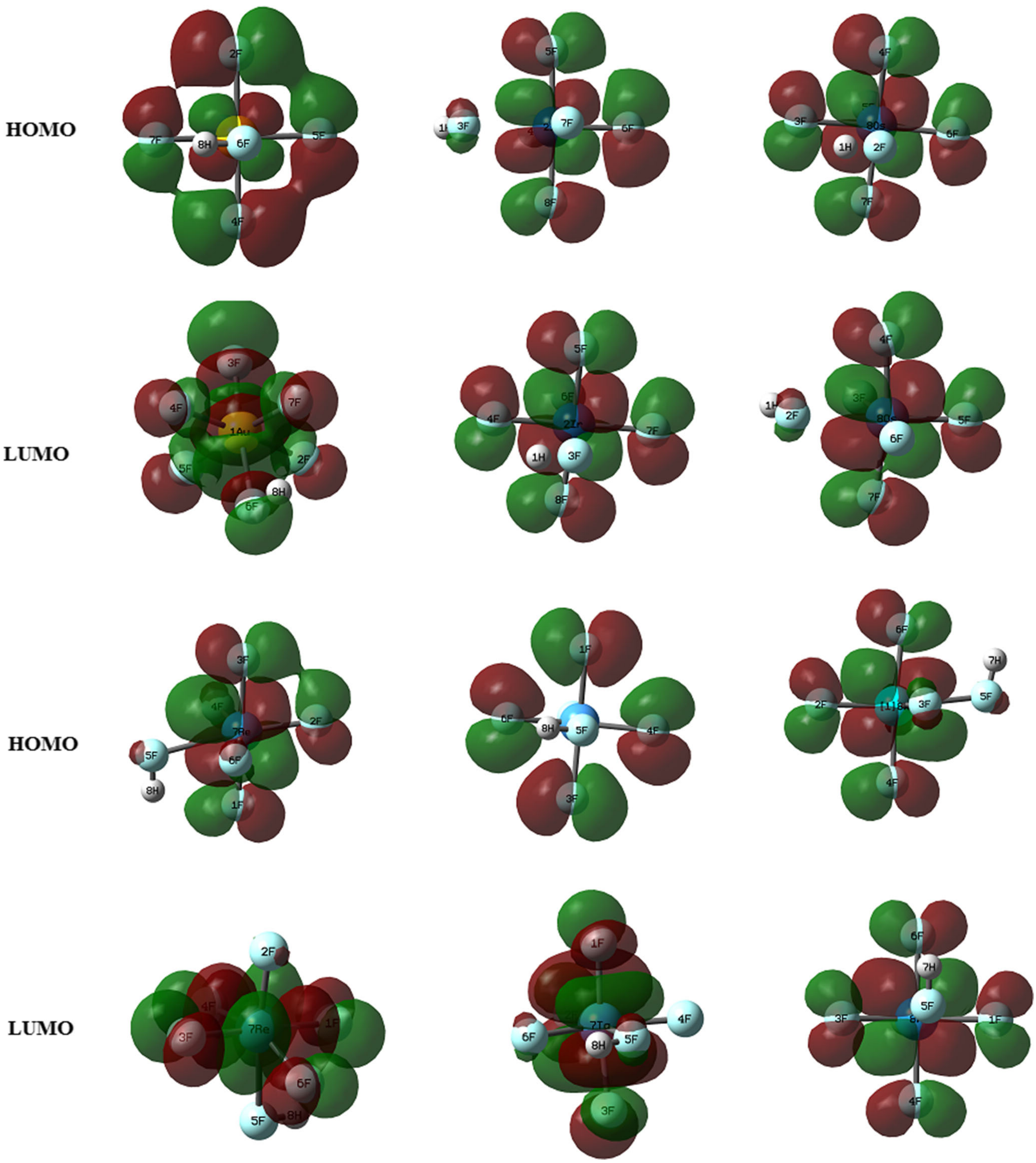

Fig. 5 HOMO-LUMO plot of hydrogenated hexafluoride

$$\Delta E_{diss} = E\ (LiMF_6) - E(MF_5) - E(LiF)$$

The calculated dissociation energy shows that these salts are stable against LiF dissociation.

The calculated HOMO-LUMO gaps of $LiMF_6$ are also presented in Fig. 6. The $LiTaF_6$ supersalt has the highest E_{gap}; however, $LiIrF_6$ has the lowest E_{gap} value. The percentage contribution of M, F, and Li atoms in LUMO and HOMO is calculated and listed in Table 5 by Gauss Sum 2.2 [45] program. The PDOS calculation shows that Li atom does

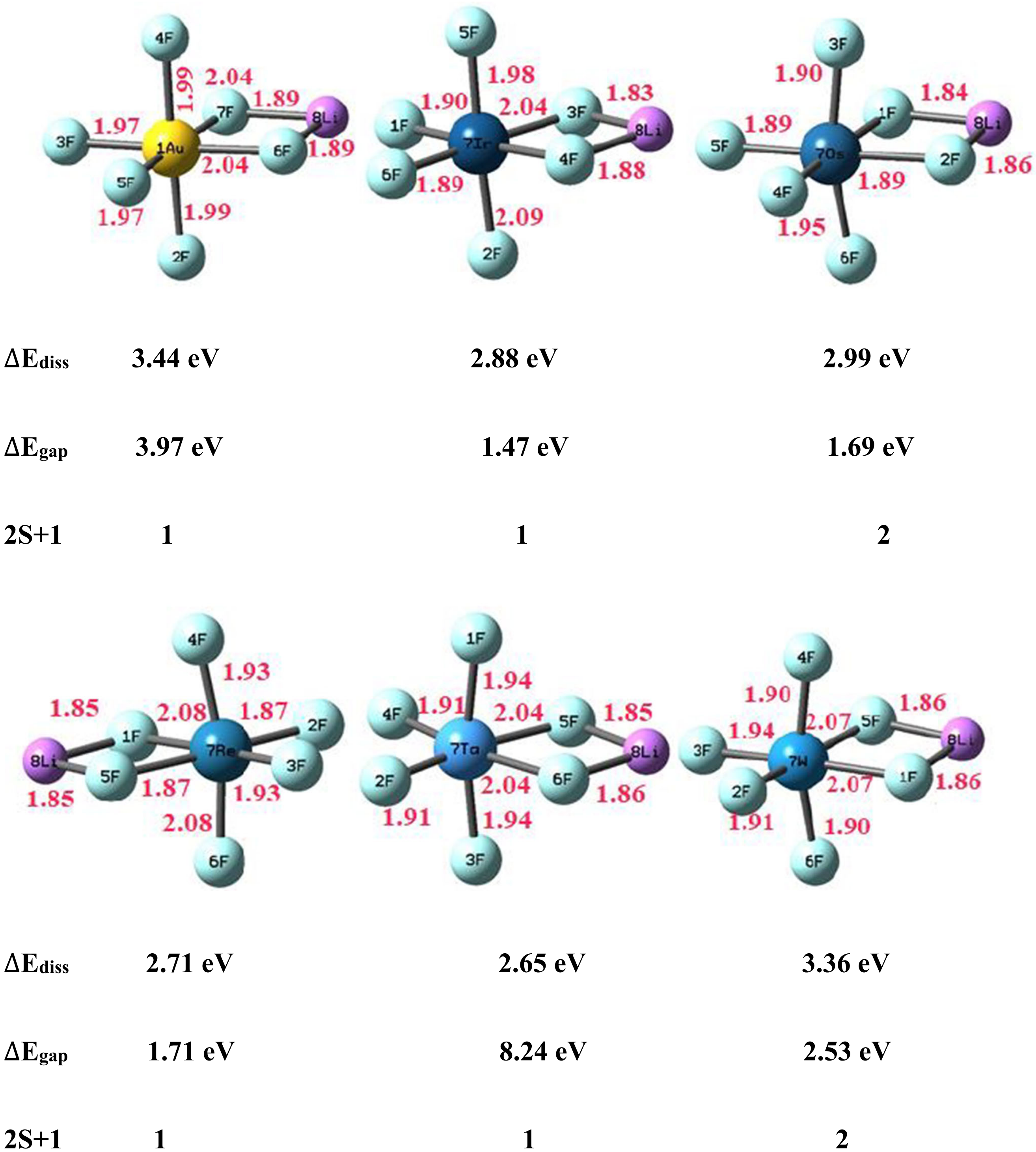

Fig. 6 Optimized structure of MF_6 along with Li salt and bond length (in A°)

not show any contribution of HOMO-LUMO plot. To know about nature of interaction, we have performed QTAIM analysis [46] of $LiMF_6$. Some topological parameters are collected in supplementary Table 5. According to Koch and Popelier criteria [44], no nonbonding interaction appeared in $LiMF_6$. According to Koch and Popelier criteria [44], bonding in $LiMF_6$ salts is electrovalent in nature [26, 47, 48] because for all interactions $\nabla^2\rho>0$, $H>0$ at BCP as in LiCl salt. The electrovalent bonding in $LiMF_6$ can also verify with NBO charge on Li in $LiAuF_6$ (0.8774e), $LiIrF_6$ (0.8443e), $LiOsF_6$

Table 5 Percentage contribution of M, F, and Li in frontier orbitals in $LiMF_6$ salts

Species	Bond length		Symmetry	Frontier orbital	% contribution		
					Li	F	M
$LiAuF_6$	Au-F	1.93–2.02	C_1	HOMO	0%	97%	3%
	Li-F	1.81		LUMO	1%	48%	50%
$LiIrF_6$	Ir-F	1.89–2.02	C_1	HOMO	0%	59%	41%
	Li-F	1.80		LUMO	0%	23%	77%
$LiOsF_6$	Os-F	1.87–2.04	C_1	HOMO	0%	α(36%), β(33%)	α(64%), β(67%)
	Li-F	1.75		LUMO	0%	α(35%), β(34%)	α(65%), β(66%)
$LiReF_6$	Re-F	1.85–2.06	C_1	HOMO	0%	30%	70%
	Li-F	1.79		LUMO	0%	16%	84%
$LiTaF_6$	Ta-F	1.89–2.05	C_1	HOMO	0%	100%	0%
	Li-F	1.78		LUMO	0%	15%	85%
$LiWF_6$	W-F	1.89–2.05	C_1	HOMO	0%	α(29%%), β(99%)	α(71%), β(1%)
	Li-F	1.79		LUMO	0%	α(13%%), β(11%)	α(87%), β(88%)

(0.8415e), $LiReF_6$ (0.8483e), $LiTaF_6$ (0.8486e), and $LiWF_6$ (0.8296e) which are nearly equal to one electron charge clear of its electrovalent character.

Conclusion

Our DFT/B3LYP method and SDD/6-311++G (d, p) basis set calculation represent the following conclusions:

1. All HMX_6 show potential candidates for superacids, as the MX_5 and HX subunits might be noted as Lewis/Brønsted superacids and the value of the gas phase Gibbs free energies of the deprotonation process for HMF_6 species are smaller than the gas phase Gibbs free energies of the deprotonation process of H_2SO_4.
2. The dissociation energy ΔE_{diss}>0 for HMF_6 through HF channel shows that all species are thermodynamically stable against dissociation through HF channel.
3. The acidity of $HAuF_6$ and $HOsF_6$ is nearly the same most acidic species $HSbF_6$.
4. The correlation factor R^2=0.93 suggests that a good correlation occurs in between acidity of HMF_6 and VDE of their conjugate superhalogen anions(MF_6^-).
5. The E_{gap} of HMF_6 are lower than E_{gap} of HF which shows that HMF_6 are chemically reactive.
6. These superacids have a strong tendency to form new class supersalts as they interact with strong base; however, PDOS calculations plots of $LiMF_6$ verify its covalent charter.

We hope that these new class of superacids may attract those synthetic chemists which are concerned with inorganic reactions. Note that our calculation on these species HMF_6 are based on their theoretical deprotonation reactions in which we are neglect various effects observed in gas phase.

Supplementary Information The online version contains supplementary material available at https://doi.org/10.1007/s11224-021-01809-8.

Code availability Licenced codes are used.

Author contribution Anoop Kumar Pandey: Most calculations and writing.
D. V. Shukla: Modelling and writing.
Vijay Narayan: Literature survey and writing.
Vijay Singh: Methods and some calculations.
Apoorva Dwivedi: Whole paper final writing and submission process (corresponding author).

Data availability Data and materials are real. First time any study is done on these aforesaid materials.

Declarations

Conflict of interest The authors declare no competing interests.

References

1. Nishikawa K, Nojima H (2001) Japan J. Appl. Phys. 40:835–837
2. Miller NJ (1984). J. Ment. Health Adm 11:36–37

3. Giri S, Bahera S, Jena P (2014) Angew Chem. Int. Ed 53:13916–13919
4. Srivastava AK, Misra N (2016). Polyhedron 117:422–426
5. Srivastava AK, Misra N (2016) Electrochem. Commun 68:99–103
6. Koppel IA, Burk P, Leito I, Sonoda T, Mishima M (2000). J. Am. Chem. Soc. 122:5114–5124
7. Hall NF, Conant JB (1927). J. Am. Chem. Soc. 49:3047–3061
8. Hogeveen H, Bickel AF (1969) Recl. Trav. Chim. Pays-Bas 88: 371–378
9. Hogeveen H, Bickel AF (1967) J. Chem. Soc. Chem. Commun. 13: 635–636
10. Gillespie RJ, Peel TE (1971) Adv. Phys. Org. Chem. 9:1–24
11. Gillespie RJ, Peel TE (1973) J. Am. Chem. Soc. 95:5173–5178
12. Olah GA, Schlosberg RH (1968) J. Am. Chem. Soc. 90:2726–2727
13. Bickel AF, Gaasbeek CJ, Hogeveen H, Oelderik JM, Platteeuw JC (1967) Chem Commun 634–635
14. Olah GA, Lukas J (1967). J. Am. Chem. Soc. 89:2227–2228
15. Olah GA, Prakash GK, Sommer J (1979) Superacids. Science 206: 13–20
16. Czapla M, Skurski P (2015). Chem. Phys. Lett. 630:1–5
17. Czapla M, Skurski P (2015). J. Phys. Chem. A 119:12868–12875
18. Srivastava AK, Misra N (2015). Polyhedron 3:277–283
19. Shukla DV, Srivastava AK, Misra N (2017). Main group chemistry 16(2):141–150
20. Czapla M, Skurski P, Anusiewicz I (2016). RSC Adv. 6:29314–29325
21. Srivastava A K, Misra N Kumar A (2017) New J Chem 41:5445–5449
22. Frisch, MJ, Trucks GW, Schlegel HB, Scuseria GE, Robb MA, Cheeseman JR, Scalmani G, Barone V, Mennucci B, Petersson GA, Nakatsuji H, Caricato M, Li X, Hratchian HP, Izmaylov AF, Bloino J, Zheng G, Sonnenberg JL, Hada M, Ehara M, Toyota K, Fukuda R, Hasegawa J, Ishida M, Nakajima T, Honda Y, Kitao O, Nakai H, Vreven T, Montgomery JA Jr, Peralta JE, Ogliaro F, Bearpark M, Heyd JJ, Brothers E, Kudin KN, Staroverov VN, Kobayashi R, Normand J, Raghavachari K, Rendell A, Burant JC, Iyengar SS, Tomasi J, Cossi M, Rega N, Millam JM, Klene M, Knox JE, Cross JB, Bakken V, Adamo C, Jaramillo J, Gomperts R, Stratmann RE, Yazyev O, Austin AJ, Cammi R, Pomelli C, Ochterski JW, Martin RL, Morokuma K, Zakrzewski VG, Voth GA, Salvador P, Dannenberg JJ, Dapprich S, Daniels AD, Farkas Ö, Foresman JB, Ortiz JV, Cioslowski J, Fox DJ (2009) Gaussian 09, revision E.01, Gaussian, Inc., Wallingford CT, 2009
23. Topol IA, Tawa GJ, Burt SK, Rashin AA (1997). J. Phys. Chem. A 101:10075–10081
24. Dennington R, Keith T, Millam J (2009) GaussView Version 5, Semichem Inc. Shawnee Mission KS
25. Macgregor SA, Moock KH (1998). Inorg. Chem. 37:3284
26. Graudejus O, Wilkinson A P, Chacon L C, Bartlett N (2000) Inorg Chem 39(13):2794–2800
27. Hoskins BF, Linden A, Mulvaney PC, O'Donnell TA (1984). Inorg.Chim. Acta 88:217
28. Fitz H, Muller BG, Graudejus O, Bartlett NZ (2002). Z. Anorg. Allg. Chem. 628:133
29. Graudejus O, Muller BGZ (1996). Z. Anorg. Allg. Chem. 622:1076
30. George PM, Beauchamp JL (1979). Chem. Phys. 36:345
31. Viggiano AA, Paulson JF, Dale F, Henchman M, Adams NG, Smith DJ (1985). Phys. Chem. 89:2264
32. Korobov MV, Kuznetsov SV, Sidorov LN, Shipachev VA, Mit'kin VN (1989). Int. J. Mass Spectrom. Ion Process. 87:13
33. Friedman JF, Stevens AE, Miller TM, Viggiano AA (2006). J. Chem. Phys. 124:224306
34. Craciun R, Picone D, Long RT, Li S, Dixon DA (2010). Inorg. Chem. 49:1056–1070
35. Gutsev GL, Boldyrev AI (1983). Chem. Phys. Lett. 101:441
36. Miyoshi E, Sakai Y, Murakami A, Iwaki H, Terashima H, Shoda T, Kawaguchi T (1988). J. Chem. Phys. 89:4193
37. Miyoshi E, Sakai Y (1988). J. Chem. Phys. 89:7363
38. Koirala P, Willis M, Kiran B, Kandalam AK, Jena P (2010). *J. Phys. Chem. C* 114:16018–16024
39. Srivastava AK, Misra N, Pandey SK (2015). Chem. Phys. Lett. 624: 15–18
40. Siddiqui SA, Rasheed T (2012) Int J Quantum Chem 113(7):959–965
41. Srivastava AK, Misra N (2014). J. Fluor. Chem. 158:65–68
42. Srivastava AK, Misra N, Pandey AK (2015). J. Chem. Sci. 127: 1853–1858
43. Czapla M, Skurski P (2017). Int. J. Quantum Chem. 25:494
44. Koch U, Popelier P (1995). J. Phys. Chem. A 99:9747–9754
45. O'boyle NM, Tenderholt AL, Langner KM (2008). J. Comput. Chem. 29:839–845
46. Keith T A, Gristmill T K Software overland park KS USA 2019.
47. Rasheed T, Siddiqui SA, Pandey AK, Bouarissa N, AliAl-Hajry (2017). J. Fluor. Chem. 195:85–92
48. Rasheed T, Siddiqui SA, Pandey AK, Mishra M (2012). J. Fluor. Chem. 135:285–291